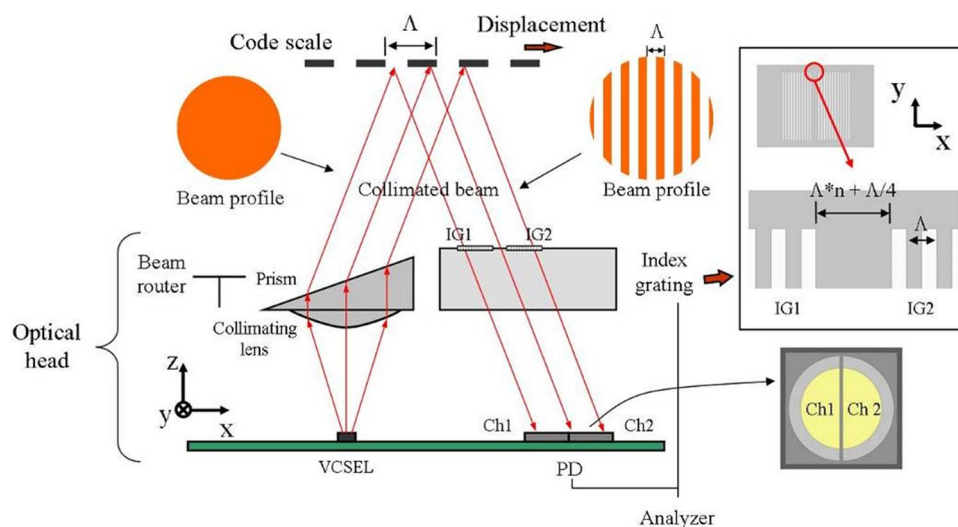


Reflective Optical Encoder Capitalizing on an Index Grating Imbedded in a Compact Smart Frame

Volume 6, Number 2, April 2014

Hak-Soon Lee
Sang-Shin Lee



DOI: 10.1109/JPHOT.2014.2307554
1943-0655 © 2014 IEEE

Reflective Optical Encoder Capitalizing on an Index Grating Imbedded in a Compact Smart Frame

Hak-Soon Lee and Sang-Shin Lee

Department of Electronic Engineering, Kwangwoon University, Seoul 139-701, Korea

DOI: 10.1109/JPHOT.2014.2307554

1943-0655 © 2014 IEEE. Translations and content mining are permitted for academic research only.

Personal use is also permitted, but republication/redistribution requires IEEE permission.

See http://www.ieee.org/publications_standards/publications/rights/index.html for more information.

Manuscript received January 6, 2014; revised February 11, 2014; accepted February 16, 2014. Date of publication February 20, 2014; date of current version March 3, 2014. This work was supported in part by the National Research Foundation of Korea (NRF) under Grant 2013-008672 funded by the Korean government (MSIP) and in part by aresearch grant from Kwangwoon University in 2014. Corresponding author: S. S. Lee (e-mail: slee@kw.ac.kr).

Abstract: A reflective optical encoder has been proposed and realized capitalizing on a miniaturized sensing head, which integrates both a pair of index gratings and a beam router in a plastic smart frame. The index gratings play a role in selectively transmitting the incident beam carrying the periodic grating pattern of a code scale. The beam router, consisting of a collimating lens in conjunction with a prism, is used to collimate and steer the beam originating from a vertical-cavity surface-emitting laser (VCSEL) toward the code scale. The proposed encoder is rigorously designed by ray optic simulations and manufactured by passively aligning a smart frame, which is produced by plastic injection molding, with a VCSEL at $\lambda = 850$ nm and two semicircular photodetectors. The index grating is created by forming an Al grating pattern of a $10\text{-}\mu\text{m}$ pitch on a silica substrate. Two output signals provide sinusoidal signals, which are 90° out of phase from each other. The period of the signals is $4\ \mu\text{s}$ at a frequency of 250 kHz, which is equivalent to a period of $10\ \mu\text{m}$. As expected, the relative phase relationship is reversed by altering the direction of rotation of the code scale. By examining either of the two output signals, we can simply demonstrate positional and angular resolutions of about $10\ \mu\text{m}$ and 0.04° , respectively. The attained resolutions can be readily enhanced to $2.5\ \mu\text{m}$ and 0.01° , by simultaneously taking into account the two signals with a distinct 90° phase difference.

Index Terms: Sensors, micro-optics, gratings, electro-optical systems.

1. Introduction

An optical encoder has become recognized as an indispensable displacement/position sensor due to its advantages of excellent immunity to electromagnetic interference, high resolution, and light weight [1]–[3]. It plays a pivotal role in a wide range of applications entailing precise position control, encompassing robotic controllers, printers, cameras, military weapons, and biosensors [4]–[9]. The encoder, which typically involves a code scale, an optical sensing head, and a signal processing circuit, is classified into two categories of reflection or transmission type depending on the arrangement of light sources, code scales, and photodetectors (PDs). Although a transmission-type encoder was usually pursued to conveniently dispose its constituent elements, it suffered from shortcomings such as bulky size and poor integration. When the encoder is built resting on an active alignment rather than a passive alignment, its cost effectiveness is critically degraded [10]–[12]. In order to produce an output signal in response to the displacement of an object, the pattern of the

code scale should be adaptively transferred, either directly to an array of small PD cells, which are elaborately disposed with a higher accuracy than the pitch of the code scale, or to a plain PD via a secondary scale pattern, serving as an analyzer [13]–[21]. Since a special version of arrayed PD cells is extremely expensive and, moreover, susceptible to limited applications, an alternative approach utilizing an analyzer is necessary.

In this paper, we construct a reflective optical encoder capitalizing on a miniaturized sensing head, which integrates both a pair of index gratings and a beam router into a plastic smart frame. The index gratings selectively transmit the incident beam mimicking the periodic grating pattern of a code scale. The beam router, consisting of a collimating lens accompanied by a prism, is used to collimate and steer the beam originating from a vertical-cavity surface-emitting laser (VCSEL) toward the code scale. The displacement of the code scale can efficiently translate into modulated electrical signals available from the two channels (Ch1 and Ch2) of semicircular PDs, which are used to embrace the incoming beam analyzed by the index gratings. The proposed encoder is rigorously designed and analyzed through ray optic simulations and then manufactured by passively aligning a smart frame, which is produced by plastic injection molding, with a VCSEL at $\lambda = 850$ nm and silicon PDs. The propagating beam is reflected by the code scale to precisely replicate its pattern and subsequently analyzed by the proposed index gratings. When the optical head is aligned to a rotary code scale, two sinusoidal waveforms, exhibiting a distinct 90° phase relationship, are produced in response to the displacement of the code scale.

2. Proposed Reflective Optical Encoder Incorporating Integrated Index Gratings and Its Design

The proposed reflection-type optical encoder, tapping into a miniaturized optical sensing head featuring a pair of index gratings and a beam router, which are embedded in a smart frame, is schematically illustrated in Fig. 1(a). The encoder is principally composed of an optical head, which is responsible for the generation, routing, and reception of light beam, and a code scale, which is used to optically encode the positional displacement to be measured. The code scale is engraved with a reflection grating with a pitch of Λ . The optical head includes a VCSEL source, a beam router which consists of a collimating lens and prism, an analyzer including a pair of gratings, and two monitoring PDs. A pair of small index gratings is specifically introduced to serve as an analyzer, by selectively allowing the light beam reflected by the code scale to be delivered to the PDs, in accordance with the displacement of the scale. The proposed analyzer comprises two transmission metallic gratings of an identical pitch Λ , IG1 and IG2, which are set apart by integer multiples of Λ plus a quarter. Two semicircular PDs are individually adopted to detect the optical power carried by the beam which is travelling past the stationary index grating, when the pattern of the reflection grating related to the code scale is shifted.

For the proposed optical encoder, the operation principle is elucidated, as shown in Fig. 1(a), based on the behavior of light rays, while the resulting output signals are depicted in Fig. 1(b). The light emitted by the VCSEL is initially collimated and successively steered by the combination of the lens and prism belonging to the beam router. The collimated beam, which is simply deemed to have a uniform profile, is periodically reflected by the grating pattern pertaining to the code scale, so as to be converted to a beam that is spatially modulated with the same period Λ . The spatially modulated beam encounters two identical index gratings of the same pitch Λ (IG1 and IG2), which are separated from each other by $(m + 1/4)\Lambda$, for $m = 0$ or positive integers. Light coming out of IG1 and IG2 finally reaches the PD corresponding to Ch1 and Ch2, respectively. The output signals for Ch1 and Ch2 are expected to exhibit a phase difference of 90° , as described in Fig. 1(b). Four representative cases of the reflected beam relative to the fixed index grating are specified in Fig. 1(b). For Case1, the incoming spatially modulated beam pattern, which results from the movement of the rotary code scale, is initially deviated from the index grating pattern of IG1 by $\Lambda/2$, thereby maximizing the optical power to be delivered to the Ch1 PD. In the meantime, the optical power for the Ch2 PD assumes a medium level, when the incident beam is offset from IG2 by $3\Lambda/4$. For Case2, where the incoming beam has been successively shifted by $\Lambda/4$, the powers for Ch1

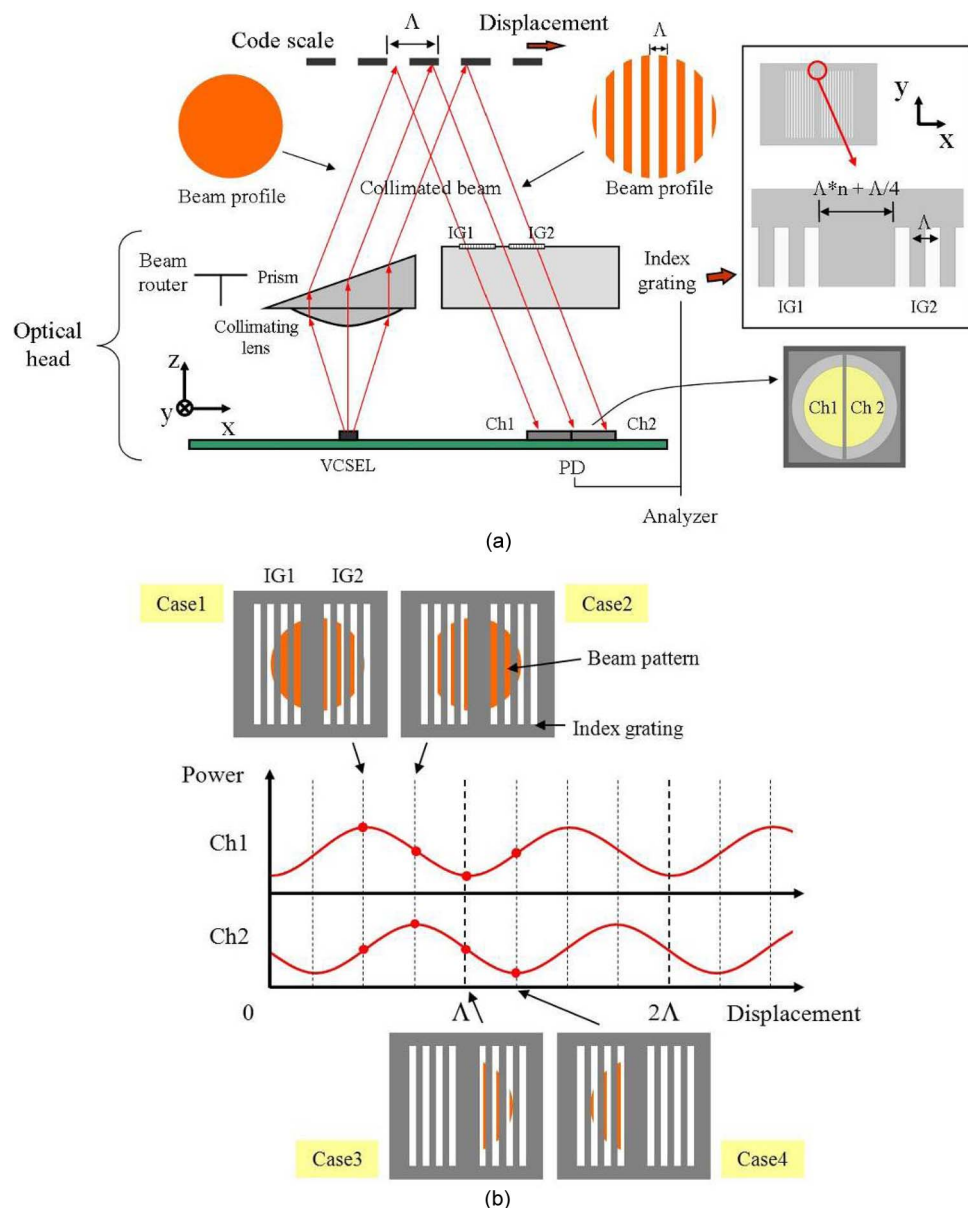


Fig. 1. Configuration of the proposed optical encoder utilizing an index grating. (a) Operation principle. (b) Output signals for different situations in terms of IG and reflected modulated beam.

and Ch2 decline and increase to medium and peak levels, respectively. With an additional $\Lambda/4$ displacement of the beam for Case3, the powers for Ch1 and Ch2 arrive at minimum and medium levels. Finally, for the situation of Case4, as a result of a subsequent $\Lambda/4$ shift of the beam, the output powers change to medium and minimum levels for Ch1 and Ch2, respectively. Eventually, the output signals produced by Ch1 and Ch2 PDs emulate two sinusoidal waveforms of a period Λ , providing a phase difference of 90° . The use of the index grating based analyzer means that the proposed encoder does not need to draw upon an array of delicately arranged small PD cells, which should be custom-made depending on the configuration of the code scale.

We conducted rigorous ray optic simulations in order to determine the structural parameters associated with the proposed sensor and then validated its performance. The outcome of the design is presented in detail in Fig. 2(a). The light source comprises a VCSEL operating at $\lambda = 850$ nm, with a divergence of 30° . The beam router containing the lens and prism is made up of polycarbonate

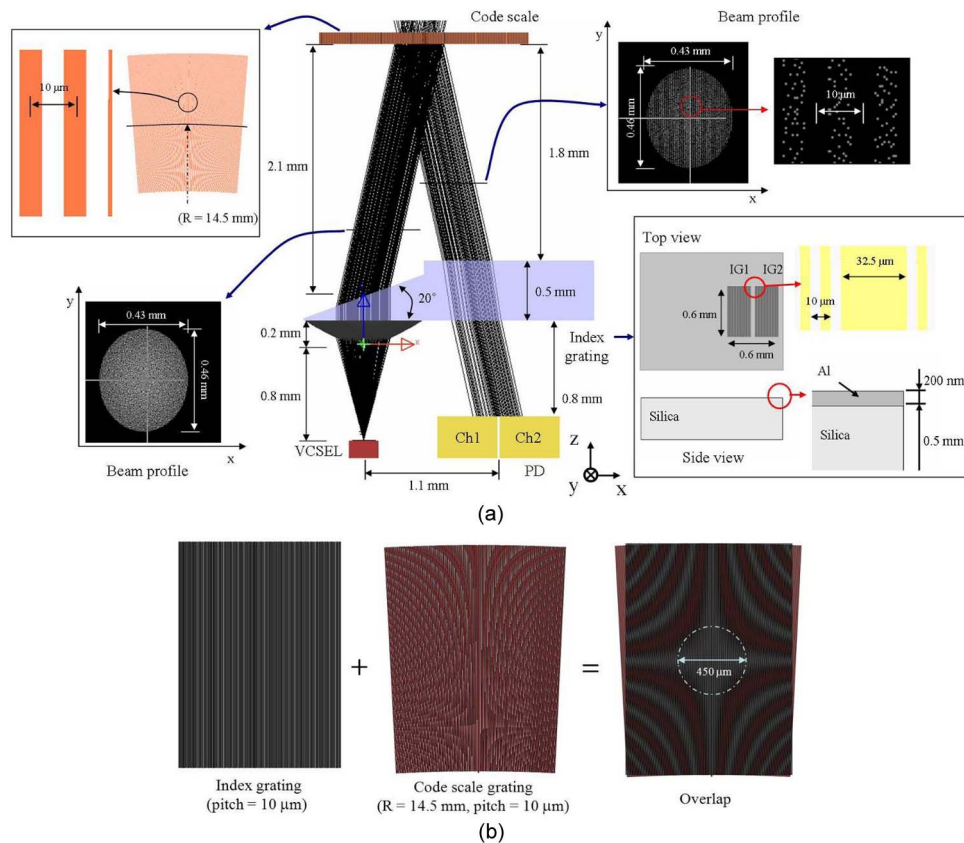


Fig. 2. (a) Designed optical encoder with structural parameters included. (b) Overlap between the grating patterns associated with the code scale and index grating.

($n = 1.586 @ \lambda = 850 \text{ nm}$). The code scale contains a reflection grating with a pitch of $\Lambda = 10 \text{ }\mu\text{m}$, engraved on a thin metallic disc of 14.5-mm radius. Similar to the case of the code scale, the index grating, acting as an analyzer, is created by forming a 200-nm-thick Al grating pattern on a 0.5-mm-thick silica substrate. We initially attempted to determine the gap between the VCSEL and lens, which controls the spot size of the collimated beam. As depicted in Fig. 2(b), a straight grating pattern, as observed in the index grating, is superimposed upon a fan-shaped grating written in the rotary code scale, signifying that an effective overlap region with a diameter of about $450 \text{ }\mu\text{m}$ can be secured. Hence, in an attempt to attain such a collimated beam with a spot size of $450 \text{ }\mu\text{m}$, the distance between the VCSEL and lens and the angle of the prism were set at 0.8 mm and 20° , respectively. Considering both the PD footprint and space for wire bonding, the center-to-center gap between the VCSEL and PD was set at 11 mm. To facilitate the acceptance of the beam emitted by the VCSEL into the PD, the distance of the prism from the code scale was set at 2.1 mm. Next, regarding the design parameters for the index grating based analyzer, the separation between the two gratings of IG1 and IG2 was set at $32.5 \text{ }\mu\text{m}$, thereby suppressing the crosstalk between Ch1 and Ch2 PDs. In light of the spot of the incident collimated beam, each of the two index gratings was designed with effective dimensions of $600 \times 300 \text{ }\mu\text{m}^2$. We confirmed that the incoming beam with a uniform profile was converted into a spatially modulated pattern with the same pitch as that of the code scale. For the designed encoder, the output signals were estimated in terms of the shift in the code scale. As plotted in the left graph of Fig. 3, two sinusoidal signals, each with a period of $10 \text{ }\mu\text{m}$, are acquired at the two channels when the code scale is rotated along the x -axis in the clockwise direction. The Ch1 signal is monitored to lead the Ch2 signal by a phase equivalent to a quarter of the pitch. In contrast, as shown in the right graph of Fig. 3, the Ch2 signal is observed to lead the Ch1 signal by the same phase, when the code scale rotates in the counter-clockwise direction.

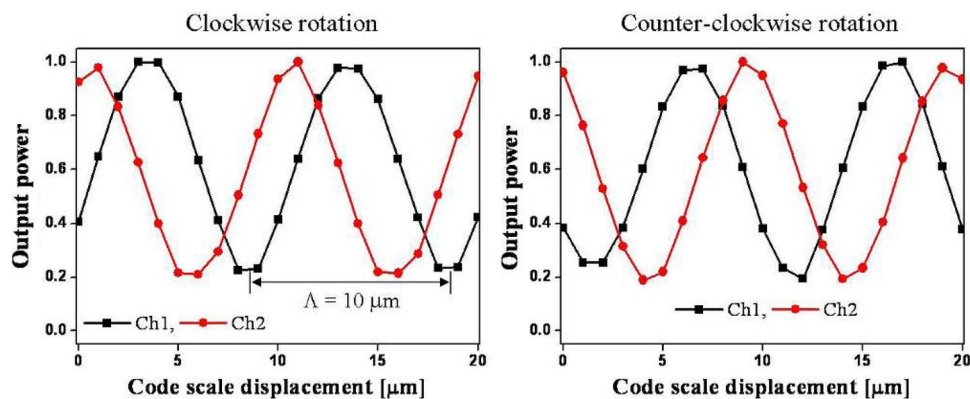


Fig. 3. Output sinusoidal signals available from the two PD channels for the cases of clockwise and counter-clockwise displacement.

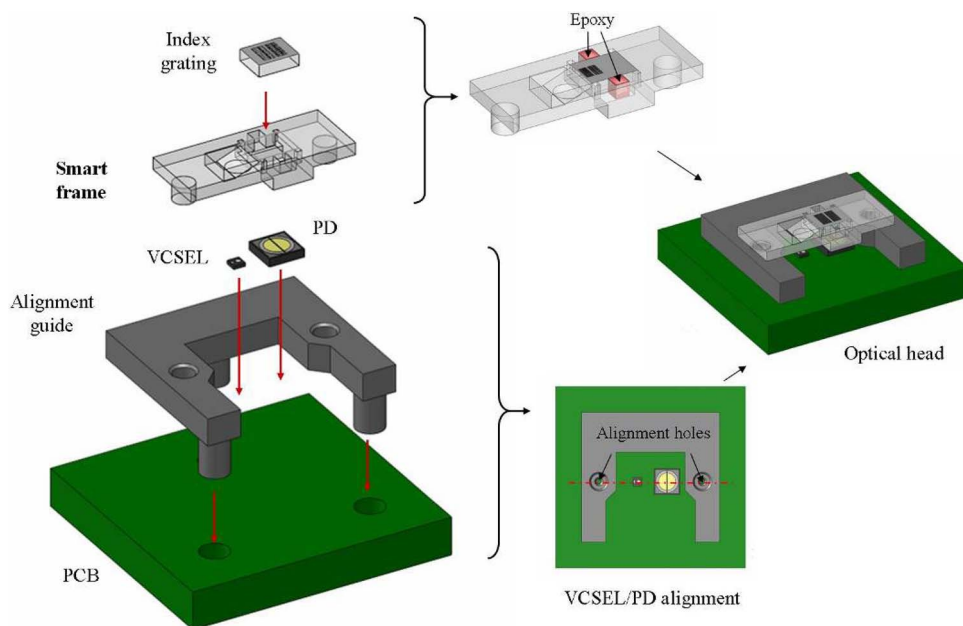


Fig. 4. Passive alignment taking advantage of the compact smart frame and alignment guide.

3. Implementation of the Proposed Optical Encoder and Its Characterization

As one of its salient features, the proposed encoder may be cost effectively built via a passive assembly process. As described in Fig. 4, the optical head was passively assembled based on a pick-and-place scheme, which is facilitated by the combination of the compact smart frame and the alignment guide. The smart frame, which plays a pivotal role in monolithically integrating the beam router that comprises the lens and prism with the index gratings, was linked to the alignment guide, so as to ensure automatic alignment of the lens, VCSEL, index gratings, and PDs altogether. The index grating substrate was installed into the smart frame and then fixed with an epoxy. The alignment guide was subsequently appended to the PCB, by matching the column of the former with the hole of the latter. After the VCSEL and PD were mounted with reference to the line connecting the built-in holes of the guide, the optical head was completed by setting the smart frame on the PCB.

The completed optical encoder is displayed in Fig. 5. As shown in Fig. 5(a), the optical head, with dimensions of $8(W) \times 7.5(L) \times 1.2(H)$ mm³, embraces the plastic smart frame for holding both the

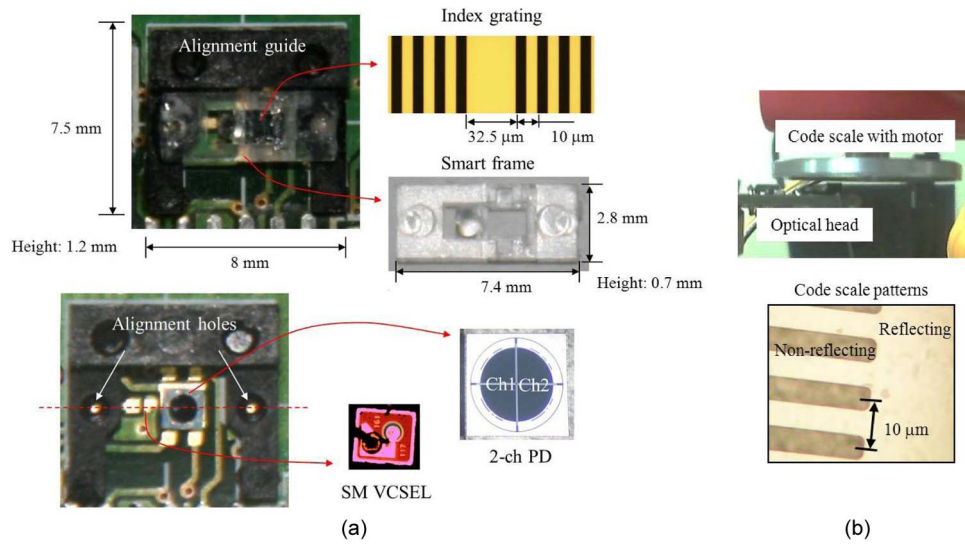


Fig. 5. (a) Constructed optical sensing head. (b) Completed displacement sensor with the scale pattern inserted.

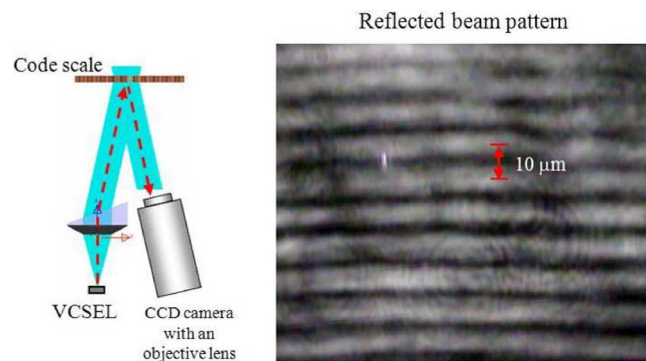


Fig. 6. Observation of reflected beam patterns.

beam router and the alignment guide, which were fabricated through a plastic injection molding technique in polycarbonate and polyimide, respectively. The collimating lens and prism belonging to the smart frame, with dimensions of $7.4(W) \times 2.8(L) \times 0.7(H)$ mm³, were visually inspected by a zoom lens based camera to confirm precise manufacture within a tolerance of 10 μm. A VCSEL at $\lambda = 850$ nm from Oclaro, USA functioned as the light source, while two semicircular silicon pin-PDs with a diameter of $D = 500$ μm were used to receive the incident beam spot of 450 μm in diameter. The left- and right-hand sections of the PD disc were respectively reserved for the output channels, Ch1 and Ch2. The periodic patterns related to the two index gratings of IG1 and IG2 were made on top of a silica substrate by forming a transmission grating with a pitch of 10 μm via lift-off process, which is made up of 200-nm-thick Al films. The separation between IG1 and IG2 was checked to be 32.5 μm, as intended. The VCSEL and PD were appropriately mounted with an accuracy of below 10 μm with respect to the reference holes. The proposed encoder was completed by aligning the optical head with the rotary code scale, which consists of a 10-μm pitch reflection grating engraved on a metallic disc. The corresponding reflectance was estimated to be above 95% and below 5% for the reflecting and non-reflecting regions, respectively.

The performance of the embodied optical encoder was thoroughly assessed by observing output signals from the two PD channels, while the profile of the beam reflected off the rotary code scale was simultaneously monitored. As revealed in Fig. 6, the reflected beam, which was directly

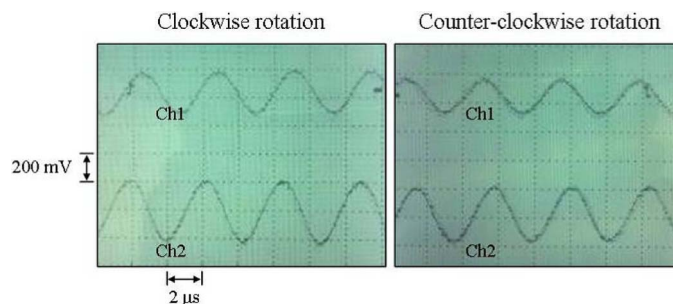


Fig. 7. Demonstrated output signals for the two PD channels for the cases of clockwise and counter-clockwise rotations.

captured by a CCD camera equipped with a zoom lens, was checked to mimic a clearly defined periodic pattern of $10\text{-}\mu\text{m}$ pitch, as predicted. With the sensor module mounted on a precision stage, the signals were monitored for Ch1 and Ch2, when the rotary code scale was driven by a motor rotating at different speeds in either clockwise or counter-clockwise direction. Fig. 7 shows the waveforms of the acquired output signals. For a signal frequency of $\sim 250\text{ kHz}$, a pair of sinusoidal signals with a desired $4\text{-}\mu\text{s}$ period was obtained, where Ch1 and Ch2 signals exhibited phase differences of positive and negative 90° for the clockwise and counter-clockwise displacements, respectively. Considering each of the channel outputs, we easily attained a positional resolution of $\sim 10\text{ }\mu\text{m}$ and an angular resolution of $\sim 0.04^\circ$. Moreover, using the 90° phase relationship between the two output channels enabled the positional and angular resolutions to be potentially enhanced to $2.5\text{ }\mu\text{m}$ and 0.01° , respectively.

4. Conclusion

We presented a compact reflection-type optical encoder that takes advantage of a passively aligned sensing head, which incorporates a miniaturized smart frame accommodating an index grating in conjunction with a beam router. The displacement of a rotary code scale was efficiently converted into a pair of output sinusoidal signals which are available from two semicircular PDs, exhibiting a 90° phase relationship, with the help of the index grating based analyzer. The attained positional resolution was ultimately better than $2.5\text{ }\mu\text{m}$.

References

- [1] K. Hane, T. Endo, Y. Ito, and M. Sasaki, "A compact optical encoder with micromachined photodetector," *J. Opt. A, Pure Appl. Opt.*, vol. 3, no. 3, pp. 191–195, May 2001.
- [2] A. Yacoot and N. Cross, "Measurement of picometre non-linearity in an optical grating encoder using x-ray interferometry," *Meas. Sci. Technol.*, vol. 14, no. 1, pp. 148–152, Jan. 2003.
- [3] H. Miyajima, E. Yamamoto, and K. Yanagisawa, "Optical micro encoder using a twin-beam VCSEL with integrated microlenses," in *Proc. 11th Int. Conf. Solid-State Sens. Actuators Transducers*, Chicago, IL, USA, 1997, pp. 1233–1235.
- [4] N. Rigoni, R. Lugones, A. Lutenberg, and J. Lipovetzky, "Design of a customized CMOS active pixel sensor for a non-diffractive beam optical encoder," in *Proc. 6th Argentine School Micro-Nanoelectron., Technol. Appl.*, Bahía Blanca, Argentina, 2011, pp. 84–88.
- [5] L. L. Dong, J. W. Xiong, and Q. H. Wan, "Development of photoelectric rotary encoders," *Opt. Precis. Eng.*, vol. 8, no. 2, pp. 198–202, 2000.
- [6] W. Yanyong, D. Fang, S. Jian, and X. Lishuan, "ANFIS parallel hybrid modeling method for optical encoder calibration," in *Proc. 24th CCDC*, 2012, pp. 1591–1596.
- [7] N. Johnson, K. J. Mohan, K. E. Janson, and J. Jose, "Optimization of incremental optical encoder pulse processing," in *Proc. iMac4s*, 2013, pp. 769–773.
- [8] L. Liang, Q. Wan, L. Qi, J. He, Y. Du, and X. Lu, "The design of composite optical encoder," in *Proc. 9th Int. Conf. Electron. Meas. Instrum.*, 2009, pp. 642–645.
- [9] K. Engelhardt and P. Seitz, "Absolute, high-resolution optical position encoder," *Appl. Opt.*, vol. 35, no. 1, pp. 201–208, Jan. 1996.
- [10] H. Miyajima, E. Yamamoto, M. Ito, S. Hashimoto, I. Komazaki, S. Shinohara, and K. Yanagisawa, "Optical micro encoder using surface-emitting laser," in *Proc. IEEE Micro Electro Mech. Syst.*, San Diego, CA, USA, 1996, pp. 412–417.

- [11] H. Miyajima, E. Yamamoto, M. Ito, S. Hashimoto, I. Komazaki, S. Shinohara, and K. Yanagisawa, "Optical micro encoder using a vertical-cavity surface-emitting laser," *Sens. Actuators A*, vol. 57, no. 2, pp. 127–135, Nov. 1996.
- [12] H.-S. Lee and S.-S. Lee, "Reflective-type photonic displacement sensor incorporating a micro-optic beam shaper," *Opt. Exp.*, vol. 22, no. 1, pp. 859–868, Jan. 2014.
- [13] J. Akedo, H. Machida, H. Kobayashi, Y. Shirai, and H. Ema, "Point source diffraction and its use in an encoder," *Appl. Opt.*, vol. 27, no. 22, pp. 4777–4781, Nov. 1988.
- [14] P. Aubert, H. J. Oguey, and R. Vuilleumier, "Monolithic optical position encoder with on-chip photodiodes," *IEEE J. Solid-State Circuits*, vol. 23, no. 2, pp. 465–473, Apr. 1988.
- [15] A. Lutenberg and F. Perez-Quintán, "Optical encoder based on a nondiffractive beam III," *Appl. Opt.*, vol. 48, no. 27, pp. 5015–5024, Sep. 2009.
- [16] N. Hagiwara, Y. Suzuki, and H. Murase, "A method of improving the resolution and accuracy of rotary encoders using a code compensation technique," *IEEE Trans. Instrum. Meas.*, vol. 41, no. 1, pp. 98–101, Feb. 1992.
- [17] J. R. R. Mayer, "High-resolution of rotary encoder analog quadrature signals," *IEEE Trans. Instrum. Meas.*, vol. 43, no. 3, pp. 494–498, Jun. 1994.
- [18] K. Engelhardt and P. Seitz, "High-resolution optical position encoder with large mounting tolerances," *Appl. Opt.*, vol. 36, no. 13, pp. 2912–2916, May 1997.
- [19] S. Wekhande and V. Agarwal, "High-resolution absolute position Vernier shaft encoder suitable for high-performance PMSM servo drives," *IEEE Trans. Instrum. Meas.*, vol. 55, no. 1, pp. 357–364, Feb. 2006.
- [20] J. Yun, J. P. Ko, J. M. Lee, and P. Nat, "An inexpensive and accurate absolute position sensor for driving assistance," *IEEE Trans. Instrum. Meas.*, vol. 57, no. 4, pp. 864–873, Apr. 2008.
- [21] D. Crespo, J. Alonso, and E. Bernabeu, "Reflection optical encoders as three-grating moiré systems," *Appl. Opt.*, vol. 39, no. 22, pp. 3806–3813, Aug. 2000.